Generation of Approximate 2D and 3D Floor Plans from 3D Point Clouds

Vladeta Stojanovic[1], Matthias Trapp[2], Rico Richter[3] and Jürgen Döllner[4]
Computer Graphics Systems Group, Hasso Plattner Institute, University of Potsdam, Germany
[1]*vladeta.stojanovic@hpi.de,* [2] *matthias.trapp@hpi.de,* [3] *rico.richter@hpi.de,* [4]*juergen.doellner@hpi.de*

Keywords: Floor Plan, 3D Point Clouds, BIM, Boundary Detection, Vector Graphics

Abstract: We present an approach for generating approximate 2D and 3D floor plans derived from 3D point clouds. The plans are approximate boundary representations of built indoor structures. The algorithm slices the 3D point cloud, combines concave primary boundary shape detection and regularization algorithms, as well as *k*-means clustering for detection of secondary boundaries. The algorithm can also generate 3D floor plan meshes based on extruding 2D floor plan vector paths. The experimental results demonstrate that approximate 2D vector-based and 3D mesh-based floor plans can be efficiently created within a given accuracy for typical indoor 3D point clouds. In particular, the approach allows for generating on-the-fly floor plan representations. It is implemented as a client-side web application, thus making it adaptable as a lightweight solution or component for service-oriented use. Approximate floor plans can be used as base data for manifold applications in various Architecture, Engineering and Construction domains.

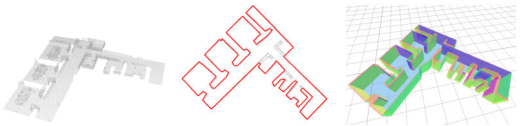

(a) (b) (c)

Figure 1: (a) Examples of floor plans for a 3D point cloud of a building's interior. (b) A 2D vector contour around the horizontal point cloud slice, and (c) an extruded 3D mesh representation of the primary 2D floor plan boundaries based on the generated vector contours.

1 INTRODUCTION

Architecture, Engineering and Construction (AEC) practitioners frequently capture the *as-is* built environment by means of 3D point clouds, which can represent, for example, both the exterior and interior of buildings. A 2D floor plan commonly provides an overview used to assess the dimensions of a room and other structural features. Floor plans can also support tasks for navigation and routing within a building, such as emergency route planning or heavy machinery management. 3D floor plans can further increase stakeholder engagement by enhancing 3D visualizations or for initial assessment of the state of the building (e.g., energy usage and capacity simulation and visualization). They can be generated by various remote-sensing and scanning approaches; 3D reconstruction based on image and video data appears to be a cost-efficient way to quickly generate an up-to-date scan of the interior of a building. By *approximate floor plans*, we refer to floor plans having limited precision, correctness, and completeness; they do not raise the claim to be architectural plans, but serve the needs of a growing number of applications that require principal information about an indoor space. (Alzantot and Youssef, 2012) generates floor plans using motion traces recorded on mobile devices, which are in turn used alongside point cloud segmentation and clustering methods to generate layouts of rooms in a building. The approach of (Okorn et al., 2010) uses voxelization of point clusters obtained from taking vertical slices of the point cloud scan to generate histograms used to detect outlines of walls, floor and ceilings for floor plan generation. Point clouds can also represent multistory indoor environments, and can be segmented and used as floor plan representations (Li et al., 2018).

Problem Statement and Approach. Our approach addresses the problem of efficiently generating approximate 2D and 3D boundary representations of building interiors from unstructured 3D point clouds. We focus on detection and evaluation of *primary* (PB) and *secondary* (SB) boundary elements; Fig. 1 illustrates examples of an approximate floor plan. The main challenges include selection of appropri-

ated point cloud vertical segmentation layers, evaluation and regularization of PBs and SBs, and generation of vector image data for use as 2D image or 3D mesh-based representations. The expected result of the approach is a 2D vector image containing regularized PB and SB evaluations of significant floor plan elements (e.g., walls, room partitions, structural elements, floors and ceilings). Additionally, a 3D mesh representation generated via extrusion of vector image paths and subsequent Boolean operations on the mesh geometry are also required. Our research addresses these challenges with the following contributions: 1) We present and discuss our method for generating concave contours of the PBs using extracted floor plan slices—by default our approach also supports generation and evaluation of convex contours. 2) We discuss the use of *k*-means clustering to detect SBs within the 2D point cloud slice where additional holes or solid features may be found (e.g., a support beam column within an open plan office). 3) We present our results for both 2D vector representations of floor plans and generated 3D floor plan meshes. The approach has been implemented as a prototypical web-based application that we used to generate experimental results. It is designed to be a lightweight solution for floor plan approximation, so it can be deployed as a web-based application or integrated as a component in a larger service-oriented architecture.

2 RELATED WORK

Boundary Rasterization. Extracting 2D and 3D boundary shapes from 3D point clouds is a challenging process—the segmentation method is key; an extensive overview of segmentation methods is given by (Nguyen and Le, 2013). The interactive indoor navigation system by (Liu et al., 2017) is based on a 3D game engine, using existing CAD floor plans and GIS maps, but does not generate floor plans for the *as-is* built environment state. However, their use of 2D CAD and GIS map data for generation of extruded 3D volumes is influential. Research by (Ambrus et al., 2017) has investigated using energy minimization, along with the *flood-filling* algorithm (Heckbert, 1990), to generate 2D floor plan projections from segmented 3D point cloud data. (Valero et al., 2012) describes a method where using maximum and minimum spatial dimensions of 3D points in the vertical plane, the ceiling and the floor planes can be extracted, and their outline can be used to further trace the contours of walls for floor plan generation. We use a similar vertical segmentation approach to select and extract horizontal point cloud slices for 2D floor plan generation, though our approach is more suited towards real-time 2D and 3D visualization, as we focus on generation of 2D vector contours and triangular 3D floor plan meshes rather than Boundary Representation Models (B-Rep) from point clouds. (Turner and Zakhor, 2014) generate simplified 2D floor plan representations, in addition to using point cloud data as basis for generating a triangulated 3D mesh that is simplified and extruded. We make use of the same 3D mesh extrusion approach, but we regularize the vector paths before extrusion to generate non-noisy 3D wall shapes (Sec. 3.4). (Previtali et al., 2014) automatically reconstructs cluttered building rooms from 3D point cloud data, where they also use cell complex labeling to construct horizontal outlines of wall shapes obtained using a binary occupancy raster map.

Point Cloud Boundary Evaluations. The Hough Transform method is a popular method for detecting vertical line segments (Ballard, 1981). While this method works well for a small number of line segments based on a number of points in a 2D image, it becomes impractical for detecting lines that include missing segments, as well as curved shapes. More flexible methods rely on the use of concave outline generation algorithms. One popular variant of this is α-shapes detection (Akkiraju et al., 1995), which is able to detect all boundary regions within a given set (including SBs), up to a certain degree of accuracy. Usage of α-shapes is basis for the α-shape algorithm, which has been described previously by (Wei, 2008) for boundary extraction of concave and convex polygons from point cloud data. We evaluate the use of the α-shape algorithm against the *Gift Opening* algorithm (Rosen et al., 2014) for PB evaluation (Sec. 3 and Sec. 4). A notable approach by (Pohl and Feldmann, 2016) is able to generate squared outlines of 2D point clouds for PB detection, in addition to detection of SBs by evaluation of distances between neighboring points. Their approach influenced our SB detection method, but instead we mostly focus on non-dense, vertically segmented 3D point clouds and finer curved boundary approximation. Research by (Ikehata et al., 2015) presents an approach for indoor modeling using a structured graph representation, where room segmentation from 3D point clouds is achieved using *k*-means clustering combined with evaluation of 2D binary and free-space coverage maps. Their use of *k*-means clustering algorithm for room segmentation and labeling inspired us to implement its use for evaluation of SBs.

Floor Plan Visualization Methods. An example of context visualization of 3D indoor models using level

of detail adaptation is described by (Hagedorn et al., 2009). In 2D representations of floor plan spaces, solid areas can be represented as lines with varying width, while in 3D visualization these contours can be extruded by using the path and widths of 2D vector lines (Feiner et al., 1990). Visualization of 2D outlines for floor plans can be realized with the use of vector graphics. The Scalable Vector Graphics (SVG) file format allows for the representation of 2D shapes in a lossless and XML-based descriptive file format, and is supported in conjunction with other web visualization standards (Duce et al., 2002). Furthermore, (Gai and Wang, 2015) discuss the development and evaluation of a web-based 3D visualization system for building floor plans, where solid 3D volumes of building floors are extruded and labeled using floor plan data stored as 2D SVG image components. We use this extrusion approach for generating the approximated 3D floor plan meshes of PBs.

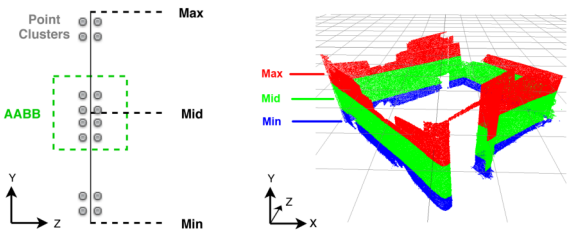

Figure 2: Selection of an appropriate vertical segmentation layer for floor plan generation using an AABB (left), sampled from the height-based segmentation of an office room 3D point cloud (right).

3 GENERATION OF FLOOR PLAN BOUNDARIES

Extraction of 2D Floor Plan Slices. We assume that the 3D point cloud scan of the building contains planar walls, which are used to partition the interior space. While the walls can be of any material or type, they must be able to be captured and represented in a 3D point cloud. We then generate the 2D horizontal point cloud layers by segmenting the 3D point cloud into three vertical levels—based on the minimum, average, and maximum height of the points in the 3D reference coordinate system. We currently select the vertical level used to generate a floor plan by computing an axis-aligned bounding box (AABB) for each of the three vertical levels, and use the level with the highest number of points in the AABB for floor plan generation (Fig. 2). We assume that the point cloud represents a standard office interior, and that it does not have any significant missing segments. For that reason, three vertical layers are sufficient for the vertical segmentation.

In most cases, however, segmented layers with higher or lower point density can be used. Outlier points are removed as they are typically points that are a certain threshold distance away from the main point cluster and are not part of dense point clusters (with respect to the overall distribution of point clusters). The maximum height of the 3D point cloud is typically based on the maximum wall height of the points in a given room scan. We can use any of the segmented layers to generate the floor plan, but usually the mid or top layers are used as they do not necessarily feature any gaps in the wall segments such as door frames (such elements can be added manually using CSG operations). Next we extract the X and Z Cartesian coordinates of the points from the segmented horizontal layer and export these as a Comma Separated Value (CSV) data file. The orientation of the 3D point cloud is set prior to extraction of the X and Z coordinates using the software tool CloudCompare (Girardeau-Montaut, 2011). CloudCompare can also be used to segmented out features such as office furniture, which are not required for the floor plan boundary approximation. Instead, we deal only with vertically segmented layers for a faster approximation of floor plan contours. A more complex approach has been implemented by (Oesau et al., 2014), which extracts horizontal slices from raw point clouds that feature the highest number of cluttered point distributions, whose computed normals are within the parallel threshold to the direction of the vertical segmentation (thus assumed to represent walls).

Concave Hull Generation and Regularization. The generation of the concave hull is accomplished using the *Gift Opening* algorithm described by (Rosen et al., 2014). The algorithm works by iterative calculation of the convex hull using the standard *Divide and Conquer* algorithm before converting the best point candidate set into a concave hull (by means of convex hull edge collapsing). We also evaluated the use of the α-shape algorithm, but found it to be too sensitive when attempting to detect narrow spaces in the 2D horizontal point cloud slices. Regularization of the concave hull requires the use of line regularization algorithms, each of which have their strengths and weaknesses when attempting regularize various elements of the concave hull. The regularization of the generated concave hull lines is accomplished by a combination of the *Douglas-Peucker* algorithm (Dou-

glas and Peucker, 1973), the *Visvalingam* algorithm (Visvalingam and Whyatt, 1993), and *radial distance simplification* (Koning, 2011). Through experimentation, we found that all three methods need to be combined to achieve a desirable line regularization result that both preserves the visual fidelity of the concave shape and simplifies noisy edges (making it suitable for floor plan contour approximation). Selection of the line simplification algorithms was established after reviewing existing implementations (Shi and Cheung, 2006), and testing the selected algorithms on 2D point cloud slices. Additionally, we evaluated each of the three regularization algorithms separately. The *radial distance simplification* method does not smooth out very noisy lines, while the *Douglas-Peucker* algorithm can over-evaluate straight line elements that have breaks in them, thus introducing dents in the line regularization. The *Visvalingam* algorithms preserves the overall shape of the the concave hull, but introduces smoother corner evaluations.

Line Path Generation. The vector line paths that form the geometric boundary representation are generated from the point set of the regularized lines. We make use of the HTML5 Canvas API to draw line strokes with varying widths, forming a line contour along each of the points. These contours are then used as the basis for the boundary representation, and can also be used as paths for extruding 3D shapes used for generating the 3D floor plan mesh. These vector contours are then exported as SVG vector paths. One disadvantage of using the SVG file format is that any geo-references contained in the original 3D point cloud must be included separately (usually as JSON data), and the corresponding SVG image must be re-projected (if specific geo-referencing is required).

3.1 Detecting SBs

One particular challenge of generating 2D vector floor plans is detecting smaller closed boundaries inside the PB of a given floor plan partition. For example, the 2D horizontal point cloud slice may contain the walls of a smaller room or region within a larger room that is not connected to the PB walls (e.g., an elevator or office cubicle), thus the resulting floor plan slice may contain what can be described as SBs. A challenge arises on how to detect these SBs to generate their regularized concave contours (Fig. 3(d)). The *Gift Opening* algorithm applied for concave generation only works on closed point sets that form a PB, and the α-shape algorithm cannot detect SBs correctly unless there is a clear distance to the PB, so we need to use a new approach. We decided to implement k-means clustering as a method to detect point regions in a 2D horizontal slice that have a higher concentration of points, and to cluster them as potential regions for SB generation (Fig. 3(a)). We do not generally sample the floor and ceiling parts of a floor plan partition for k-means clustering that contain homogeneous and continuous distributions of points, as there would be no distinguishable concentration of point clusters. The k-means cluster that contains the highest number of points is assumed to be the cluster that contains points representing the SB. The number of k-means clusters is set as the number of secondary boundaries plus one (SBs are determined visually prior to approximation, though other methods exist to heuristically determine a number of required clusters (Birodkar and Edla, 2014)). This is described in Alg. 1 as the *GenerateSecondaryBounds* function, which passes in the point set from the current k-means cluster of a floor plan partition where the SB is located, along with the PB line segments.

SB Evaluation Implementation. Alg. 1 first computes the average distance between all the points in the cluster with the *AvgDist* function call. This function randomly samples a given percentage of the points in the given cluster (taken as 75%, though this is can be adjusted if required), and returns the average distance between them. We then obtain the 2D coordinates of the current k-means center point from a given cluster with the *CenterPoint* function call. This distance value *Dist* is tested to see if it is smaller than the average point distance, so that outlier points from the cluster are not used for the SB computation. This test is performed in addition to test if the given point is within the previous boundary polygon. In the first instance of the *GenerateSecondaryBounds* function call, this previous boundary polygon is the PB polygon, but with subsequent calls to *GenerateSecondaryBounds* the previous boundary becomes the last SB to be computed. This is used to refine the SB to a satisfactory boundary shape as determined by the user. The function *PointIsInPolygon* is used for checking if the point is inside or outside of a polygon. This function casts a ray that is projected horizontally from a given point, and the number of intersections with the edges of the boundary polygon are detected as a switchable Boolean statement. To generate the SB contour, we make use of the *isPointInStroke* HTML5 Canvas API function to select only the innermost points of the SB (Fig. 3(b) and Fig. 3(c)). We use a stroke thickness of ten pixels for each of the polygon lines that the points are tested against (Alg. 2). This pixel size captures most points in a line segment (minimum three pixels width).

```
GenerateSecondaryBounds (Points, Polygon)
Result: Returns SB polygon
begin
    Points_average ← AvgDist(Points)
    Point_center ← CenterPoint(Points)
    for i ← 0 to length(Points) do
        Dist ← SqrDist(Points_i, Point_center)
        if PointIsInPolygon(Points_i, Polygon)
          then
            if Dist < Points_average then
                GenBoundary(Points_i)
            end
        end
    end
end
```

Algorithm 1: GenerateSecondaryBounds function definition.

```
GenBoundary (Points)
Result: Returns SB points
begin
    conBoundary ←
      GenerateConcaveBoundary(Points)
    conBoundary ←
      RegularizeBoundary(conBoundary)
    lineWidth ← 10
    secondaryBoundaryShape
    for i ← 0 to length(conBoundary) do
        lineTest ←
          Line(conBoundary_i, conBoundary_i+1)
        for j ← 0 to length(Points) do
            if
              isPointInStroke(Points_j, lineTest) =
              FALSE then
                secondaryBoundaryShape ←
                  Points_j
            end
        end
    end
end
```

Algorithm 2: GenBoundary function definition.

3.2 Floor Plan Boundary Visualization

We export our generated floor plan images from HTML5 Canvas image frames to SVG images prior to generation of 3D meshes from the encoded vector paths. We focus on using the SVG file format since it is supported by Three.js for 3D vector path extrusion, but other popular vector-based image formats that could also be used include Shapefiles and JSON-encoded vector data. The Three.js framework is used

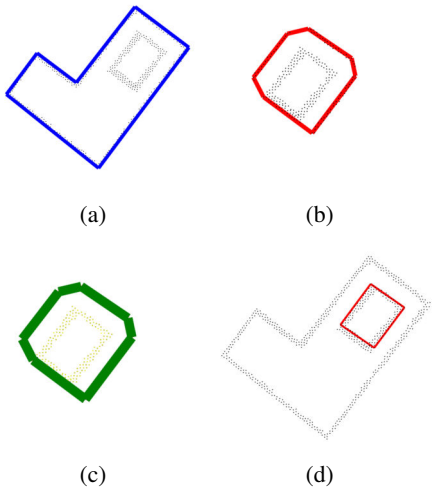

Figure 3: SB detection and generation: (a) The SB region defined by a cluster of points, contained within the PB region (blue outline). (b) Using k-means clustering the SB region is separated as a unique cluster. (c) Generated, regularized concave boundary, including points from the PB that need to be removed. (d) Boundary generated after all innermost points of the SB are detected using the same Gift Opening concave evaluation as for the PBs.

for web-based 3D visualization (Cabello et al., 2010) and, in particular, to extrude 3D geometry from SVG paths. This way, we extrude the PB as 3D mesh based on the height of the walls from the original 3D point cloud. Three.js also supports *Constructive Solid Geometry* (CSG) operations on geometry, thus we can carve out the 3D volume with any SB volumes using Boolean geometry operations. Three.js can perform CSG operations with an extension called Three-CSG.js, based on Binary Space Partitioning (BSP), where each triangular mesh used as a primitive is first converted to a BSP node (Prall, 2012). The BSP tree is then traversed and the new polygon faces are approximated using polygon splitting—where each vertex belonging to each edge of of polygon is tested to see if it is inside, outside, or co-planar to the next polygon in the hierarchy. The Boolean operations of subtraction, addition, and union of elements are represented as a series of function calls, which clip and invert each polygon in the BSP hierarchy to approximate the final CSG result. This allows us to generate 3D floor plans with variable wall thicknesses and interior SB areas that are not connected to the primary wall boundary geometry. While the CSG computation method is non-optimal, it was evaluated as a proof of concept for generating 3D meshes with secondary boundaries.

4 EXPERIMENTAL RESULTS

We have tested our approach with four different floor plan data sets. The criteria for a desirable result based on our floor plan generation can be defined as: 1) The generated PBs and SBs preserve the visual fidelity of the regularized concave contours. 2) Any expected SBs are detected and included either as a primitive that will be added, subtracted or merged (union) with the PB during CSG evaluation when generating the 3D mesh, or they are treated as independent boundaries in the 3D mesh representation. 3) The generated 3D mesh extrusion follows the extrusion paths of the vector paths contained in the generated 2D floor plan. The first two data sets, *Hallway_1* and *Hallway_2* (containing 1 799 and 1 630 points each), are used to test the PB detection and feature both regular and curved wall segments. The other four data sets, *Room_1a*, *Room_1b*, *Room_2* and *Room_3*, are used to test the SB detection (each containing 628, 605, 492, and 238 points).

The floor plans and room segments were obtained from an actual 3D point cloud from a typical office building scanned using portable LiDAR scanner. The complete 3D point cloud of segmented building interiors are down-sampled between 20 000 to 50 000 points per approximately 50 square meters using uniform sampling. For tests, such as those for the SB detection and curved surfaces, the point cloud clusters were artificially added. We have also evaluated our PB and SB detection method against the generated boundary detection using the α-shape algorithm. The criteria for the α value was the smallest value with which the SB is visually completely detected and separated from the primary bounds. The presented results in Fig. 4-5 show two different versions of a floor plan, one with straight walls and another with an artificially added curved wall section. The results were computed using a floor plan slice selected from the mid-level height of the 3D point cloud scan. The PB was computed using a three pass filtering combination of *radial distance simplification*, *Douglas-Peucker* and *Visvalingam* algorithms. The epsilon value used for the *radial distance simplification* and *Douglas-Peucker* regularization parameter was 2.4, while the epsilon value for the *Visvalingam* regularization parameter was 0.2.

The results for the SB detection presented in Fig. 6 were compared against results generated using the α-shape algorithm. The epsilon values for the combined passes of the *Douglas-Peucker* and the *radial distance simplification* algorithms were between $5.0 - 10.0$, while the epsilon value for the α-shape algorithm was set to 150.0. An additional comparison including regularization of the α-shape with a default epsilon value of 10.0 is also included. We also present initial results for the generation of non-optimized 3D meshes via CSG and vector path extrusion operations. The 3D meshes are generated and visualized using the Three.js 3D web development framework. We first present 3D mesh visualization results featuring regularized primary boundaries of a floor plan (Fig. 7). We also include results featuring extruded 3D geometry with subtracted geometry elements representing the regularized SB of a floor plan partition (Fig. 8). The geometric complexities of the generated and non-optimized 3D meshes are: Hallway_1: 137 106 vertices, 45 702 faces; Hallway_2: 93 204 vertices, 31 068 faces; Room_1a: 34 386 vertices, 11 462 faces; and Room_2: 45 102 vertices, 15 034 faces. In terms of performance, we have measured preliminary computation performance of our PB and SB generation approaches. Generation of an SB takes an average of 169 milliseconds, and the generation of PBs takes and average of 10.25 milliseconds. For the PB generation (using the *Hallway_1* and *Hallway_2* data sets), we did not partition the horizontal floor plan slice. For the SB generation tests we used two *k*-clusters for the slice partitioning, and detection of regions where the SB points are located. The development PC used features an Intel Core i5-6500 CPU at 3.2GHz, 8GB RAM and an NVIDIA GeForce GT 630 GPU (2GB of dedicated video memory), running Firefox 62.0.2.

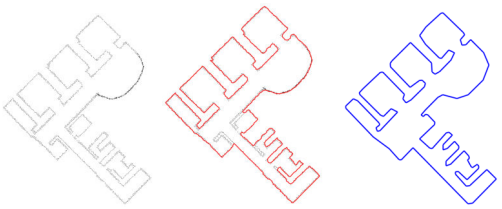

(a) (b) (c)

Figure 4: Results of the PB generation for *Hallway_1* floor plan, featuring a curved wall segment. (a) The input horizontal point cloud slice. (b) Generated non-regularized concave shape. (c) Regularization of the concave outlines.

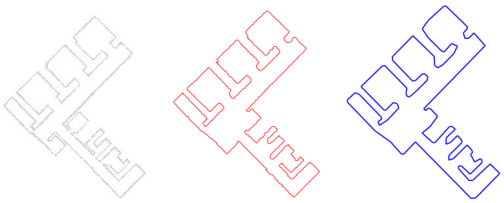

(a) (b) (c)

Figure 5: Results of the PB generation for *Hallway_2* floor plan, featuring a straight wall segments. (a) The input horizontal point cloud slice. (b) Generated non-regularized concave shape. (c) Regularized concave outlines.

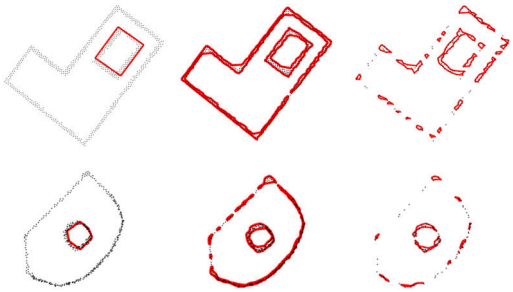

Figure 6: SB detection using our approach (left), compared to SB detection using the α-shape algorithm (center), and the α-shapes with regularization (right). Our method epsilon value: 10.0, α-shape epsilon value: 150.0, α-shape with regularization epsilon value of 10.

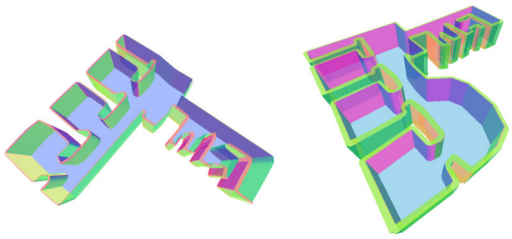

(a) (b)

Figure 7: 3D meshes of data sets *Hallway_1* and *Hallway_2*, generated from regularized primary boundaries. (a) A generated 3D mesh featuring square elements. (b) A generated 3D mesh featuring a curved wall.

5 DISCUSSION AND CONCLUSIONS

The results show that our approach is suited for generating approximate 2D and 3D floor plans of particular indoor building areas (result criteria outlined in Sec. 4), making it suitable to quickly approximate spatial dimensions, and create basis visualization data for enhancing communication and decision for AEC operations. We have compared our PB and SB evaluation method for generating 2D floor plan representations against the outputs of the α-shape algorithm. While the α-shape algorithm is able to detect SB regions with better accuracy, it suffers from over-evaluation of less dense regions. Regularization of the α-shape result also does not provide more accurate evaluation of SBs, in terms of visual quality. The *Gift Opening* algorithm for concave boundary detection works best for closed regions formed by points with similar distances between them. This becomes a problem when dealing with incomplete wall segments obtained from 3D point clouds as the algorithm will treat the missing walls segments as a concave opening.

The evaluated line regularization algorithms provide best results if they are combined, though sharp

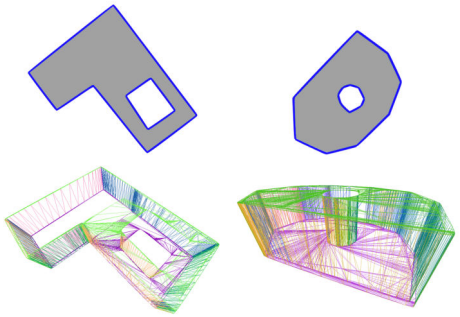

(a) (b)

Figure 8: Generated 3D meshes from regularized secondary boundaries. (a) *Room_1a*: 3D mesh featuring SB in the form of a hollow square. (b) *Room_2*: 3D mesh featuring an curved PB with a curved and hollow SB.

corners are not preserved unless a low regularization epsilon value is used. The regularization parameters are adjusted according to the density of the point cloud, i.e., evaluated as the average distance between points. There is difficulty using our approach for detecting very narrow spaces as PBs for a horizontal floor plan slice; however, they can be approximated as SBs. Notably, the α-shapes algorithm is better suited for detecting narrow spaces as PBs. SBs can be added or subtracted to the PB mesh using CSG Boolean operations, though the generated 3D meshes increase in geometric complexity and may need to be optimized. We predict approaches based on machine-learning to be applicable for floor plan generation and evaluation scenarios, thus this is also currently being investigated. The outcomes presented here contribute to the ongoing research concerning automated semantic enrichment of point clouds using a service-oriented approach (Stojanovic et al., 2018), (Discher et al., 2018).

Acknowledgments. This work was partially funded by the Research School on *Service-Oriented Systems Engineering* of the Hasso Plattner Institute.

REFERENCES

Akkiraju, N., Edelsbrunner, H., Facello, M., Fu, P., Mucke, E., and Varela, C. (1995). Alpha shapes: definition and software. In *Proceedings of the 1st International Computational Geometry Software Workshop*, volume 63, pages 66–70.

Alzantot, M. and Youssef, M. (2012). Crowdinside: automatic construction of indoor floorplans. In *Proceedings of the 20th International Conference on Advances in Geographic Information Systems*, pages 99–108. ACM.

Ambrus, R., Claici, S., and Wendt, A. (2017). Automatic room segmentation from unstructured 3-d data of in-

door environments. *IEEE Robotics and Automation Letters*, 2(2):749–756.

Ballard, D. H. (1981). Generalizing the hough transform to detect arbitrary shapes. *Pattern recognition*, 13(2):111–122.

Birodkar, V. and Edla, D. R. (2014). Enhanced k-means clustering algorithm using a heuristic approach. *Journal of Information and Computing Science*, 9(4):277–284.

Cabello, R. et al. (2010). Three. js. *URL: https://github.com/mrdoob/three. js*.

Discher, S., Richter, R., and Döllner, J. (2018). A scalable webgl-based approach for visualizing massive 3d point clouds using semantics-dependent rendering techniques. In *Proceedings of the 23rd International ACM Conference on 3D Web Technology*, page 19. ACM.

Douglas, D. H. and Peucker, T. K. (1973). Algorithms for the reduction of the number of points required to represent a digitized line or its caricature. *Cartographica: The International Journal for Geographic Information and Geovisualization*, 10(2):112–122.

Duce, D., Hopgood, B., and Lightfoot, D. (2002). Svg and x3d: Technology for a foundation course. In *Eurographics/ACM SIGGRAPH Workshop on Computer Graphics Education, Support for Computer Graphics Educators, Bristol University, UK*.

Feiner, S., Foley, J., van Dam, A., and Hughes, J. (1990). Computer graphics: Principles and practice. *Adison Wesley*.

Gai, M. and Wang, G. (2015). Indoor3d: a webgl based open source framework for 3d indoor maps visualization. In *Proceedings of the 20th International Conference on 3D Web Technology*, pages 181–187. ACM.

Girardeau-Montaut, D. (2011). Cloudcompare-open source project. *OpenSource Project*.

Hagedorn, B., Trapp, M., Glander, T., and Dollner, J. (2009). Towards an indoor level-of-detail model for route visualization. In *Proceedings of the 2009 Tenth International Conference on Mobile Data Management: Systems, Services and Middleware*, MDM '09, pages 692–697. IEEE Computer Society.

Heckbert, P. S. (1990). A seed fill algorithm. In GLASSNER, A. S., editor, *Graphics Gems*, pages 275 – 277. Morgan Kaufmann, San Diego.

Ikehata, S., Yang, H., and Furukawa, Y. (2015). Structured indoor modeling. In *Proceedings of the IEEE International Conference on Computer Vision*, pages 1323–1331.

Koning, E. d. (2011). Polyline simplification. *URL: https://www.codeproject.com/Articles/114797/Polyline-Simplification*.

Li, L., Su, F., Yang, F., Zhu, H., Li, D., Zuo, X., Li, F., Liu, Y., and Ying, S. (2018). Reconstruction of three-dimensional (3d) indoor interiors with multiple stories via comprehensive segmentation. *Remote Sensing*, 10(8):1281–1311.

Liu, K., Motta, G., Tunçer, B., and Abuhashish, I. (2017). A 2d and 3d indoor mapping approach for virtual navigation services. In *Service-Oriented System Engineering (SOSE), 2017 IEEE Symposium on*, pages 102–107. IEEE.

Nguyen, A. and Le, B. (2013). 3d point cloud segmentation: A survey. In *Robotics, Automation and Mechatronics (RAM), 2013 6th IEEE Conference on*, pages 225–230. IEEE.

Oesau, S., Lafarge, F., and Alliez, P. (2014). Indoor scene reconstruction using feature sensitive primitive extraction and graph-cut. *ISPRS Journal of Photogrammetry and Remote Sensing*, 90:68–82.

Okorn, B., Xiong, X., Akinci, B., and Huber, D. (2010). Toward automated modeling of floor plans. In *Proceedings of the symposium on 3D data processing, visualization and transmission*, volume 2.

Pohl, M. and Feldmann, D. (2016). Generating straight outlines of 2d point sets and holes using dominant directions or orthogonal projections. In *Proceedings of the 11th Joint Conference on Computer Vision, Imaging and Computer Graphics Theory and Applications: Volume 1: GRAPP*, pages 59–71.

Prall, C. (2012). Threecsg.js. *URL: https://github.com/chandlerprall/ThreeCSG*.

Previtali, M., Barazzetti, L., Brumana, R., and Scaioni, M. (2014). Towards automatic indoor reconstruction of cluttered building rooms from point clouds. *ISPRS Annals of Photogrammetry, Remote Sensing & Spatial Information Sciences*, 2(5):281–288.

Rosen, E., Jansson, E., and Brundin, M. (2014). Implementation of a fast and efficient concave hull algorithm. *Uppsala Univ*.

Shi, W. and Cheung, C. (2006). Performance evaluation of line simplification algorithms for vector generalization. *The Cartographic Journal*, 43(1):27–44.

Stojanovic, V., Trapp, M., Richter, R., and Döllner, J. (2018). A service-oriented approach for classifying 3d points clouds by example of office furniture classification. In *Proceedings of the 23rd International ACM Conference on 3D Web Technology*, Web3D '18, pages 2:1–2:9. ACM.

Turner, E. and Zakhor, A. (2014). Floor plan generation and room labeling of indoor environments from laser range data. In *2014 International Conference on Computer Graphics Theory and Applications (GRAPP)*, pages 1–12. IEEE.

Valero, E., Adán, A., and Cerrada, C. (2012). Automatic method for building indoor boundary models from dense point clouds collected by laser scanners. *Sensors*, 12(12):16099–16115.

Visvalingam, M. and Whyatt, J. D. (1993). Line generalisation by repeated elimination of points. *The cartographic journal*, 30(1):46–51.

Wei, S. (2008). Building boundary extraction based on lidar point clouds data. *Proceedings of the International Archives of the Photogrammetry, Remote Sensing and Spatial Information Sciences*, 37:157–161.